siRNAs targeting a chromatin-associated RNA induce its transcriptional silencing in human cells

Julien Ouvrard[1,2], Lisa Muniz[1,2], Estelle Nicolas[1,2]*, Didier Trouche[1,2]§*

[1]MCD, Centre de Biologie Integrative (CBI), University of Toulouse, CNRS, UPS, Toulouse, France

[2]Equipe labellisée Ligue Contre le Cancer, Team « Chromatin and Cell Proliferation », Toulouse, France

*** These authors contributed equally to this work**

Running head : Silencing of a nuclear RNA by siRNAs

Keywords: siRNA, RNA interference, nuclear RNA, transcriptional silencing

§ Correspondence to :

Didier Trouche

MCD UMR 5077, Centre de Biologie Intégrative

Université Paul Sabatier

118 Route de Narbonne

31062 Toulouse Cedex, France

E-mail : didier.trouche@univ-tlse3.fr

Abstract

Transcriptional gene silencing by small interfering RNAs (siRNAs) has been widely described in various species, such as plants or fission yeasts. In mammals, its extent remained somewhat debated. Previous studies showed that siRNAs targeting gene promoters can induce the silencing of the targeted promoter, although the involvement of off-target mechanisms was also suggested. Here, by nascent RNA capture and RNA Pol II ChIP, we show that siRNAs targeting non coding RNAs that are mainly localized in chromatin induce their transcriptional silencing. Moreover, by deleting the targeted sequence on the two alleles of one of these siRNAs by genome edition, we further found that this silencing is due to base pairing of the siRNA to the target. By using cells in which the deletion of the targeted sequence is heterozygous, we show by allele-specific RT-qPCR that only the wild type allele, but not the deleted allele, is silenced by the siRNA, indicating that transcriptional silencing occurs only in cis. Finally, we demonstrate that both Ago1 and Ago2 are involved in VINK transcriptional silencing. Altogether, our data demonstrate that siRNAs targeting chromatin-associated RNAs at distance from their promoter induce their gene silencing. Our results thus extend the possible repertoire of endogenous or exogenous interfering RNAs.

Introduction

RNA interference (RNAi), first discovered in plants during the 1990s and observed later in other systems, like worms, yeast and mammals is a rapid and efficient tool to induce the knockdown of specific transcripts. This main mechanism of post-transcriptional gene silencing is largely conserved throughout evolution. In mammals and non-mammalian organisms, exogenous or endogenously synthetized small double-stranded RNA molecules of 19 to 24 nucleotides, called small-interfering RNA (siRNA), are loaded on the RISC (RNA-induced silencing complex) complex containing argonaute proteins (Ago) (Martinez et al. 2002). The two strands of siRNAs are then dissociated and the passenger strand is ejected. The complex is then tethered to target RNAs containing a sequence complementary to the guide strand. When sequence complementarity is high enough, the endoribonuclease activity present in Ago2 cleaves the target RNA between bases 10 and 11 of the siRNA complementary region, leading to the degradation of the target RNA (Liu et al. 2004; Meister et al. 2004).

Given that the above-described processes usually take place in the cytoplasm, RNA interference is in this respect a cytoplasmic process functioning at a post-transcriptional level, and leading to RNA degradation. Nevertheless, in some organisms such as yeast or plants, RNAi has been described to work also in the nucleus to silence repeated elements and to nucleate heterochromatin, which produce low levels of double-stranded RNAs (Castel and Martienssen 2013). In this case, the RISC complex is tethered to chromatin by siRNA base pairing to the nascent targeted RNA, leading to localized heterochromatin formation and epigenetic silencing. Interestingly, a mechanism allowing the 5' extension and amplification of the RNAi response has been described. For instance in fission yeast, Ago1 protein when tethered to nascent RNA

by siRNA base pairing recruits a RNA-dependent RNA polymerase that produces an antisense RNA to the nascent RNA, thus generating double stranded RNA further processed by Dicer into new siRNAs (Castel and Martienssen 2013).

The presence of the nuclear RNAi in mammals is more controversial. Indeed, initial data concluded that intronic sequences cannot be targeted with RNAi (Zeng and Cullen 2002; Vickers et al. 2003). This observation together with the findings that some RISC proteins were mostly cytoplasmic and that RNA-dependent RNA polymerase does not exist in mammals, led to the conclusion that RNA interference is restricted to the cytoplasm in human cells (Zeng and Cullen 2002). However, in the last two decades, various studies have suggested the presence and the action of the RNAi machinery in the nucleus of mammalian cells. Indeed, whereas siRNA loading factors into RISC are exclusively cytoplasmic, other RNAi factors, such as Dicer, Ago1 and Ago2, have been found in the nucleus and can lead to the siRNA-mediated cleavage of chromatin-associated RNAs (Gagnon et al. 2014; White et al. 2014; Kalantari et al. 2016). Moreover, the preferential nuclear localization of Ago2 has been evidenced in specific human tissues (Sharma et al. 2016). It was later found that Ago-miRNA complexes can target and silence post-transcriptionally thousands of pre-mRNAs in the nucleus in mouse ES cells that contain high levels of nuclear Ago proteins (Sarshad et al. 2018; Di Fazio et al. 2022). Moreover, siRNAs have been successfully used to inhibit nuclear ncRNAs(Gagnon et al. 2014), including by ourselves (Lazorthes et al. 2015; Muniz et al. 2017; Muniz et al. 2021).

In addition, transcriptional gene silencing by siRNAs was also reported in mammalian cells. siRNAs directed against the promoter of the elongation factor 1α gene repress the expression of a reporter gene driven by this promoter (Morris et al. 2004). Further studies confirmed for other genes that siRNAs can repress transcription when targeting promoters (Castanotto et al. 2005; Janowski et al. 2005; Suzuki et al. 2005; Ting et al. 2005; Zhang et al. 2005; Janowski et

al. 2006; Weinberg et al. 2006; Napoli et al. 2009) or first exons (Stojic et al. 2016). This was also extended to miRNAs targeting downstream regions of protein-coding genes (Yue et al. 2010; Younger and Corey 2011). Transcriptional gene silencing requires an RNA template (Han et al. 2007; Hawkins et al. 2009), such as promoter-associated antisense transcripts (Schwartz et al. 2008) or ncRNAs overlapping the gene promoter or downstream regions (Napoli et al. 2009; Chu et al. 2010) and involves either Ago1 or Ago2 (Janowski et al. 2006; Kim et al. 2006; Chu et al. 2010). The targeting of the siRNA to promoters leads to the deposition of repressive chromatin marks at these promoters, such as H3K9me3 and H3K27me3 (Ting et al. 2005; Kim et al. 2006; Weinberg et al. 2006; Giles et al. 2010; Benhamed et al. 2012; White et al. 2014) or CpG methylation (Castanotto et al. 2005; Suzuki et al. 2005), resulting in transcriptional gene repression. Note that it was proposed that the previously reported transcriptional repression by siRNAs of the VEGF gene promoter and HIV LTR could be due to off-target effects, since a similar effect was observed on reporter systems with a deleted or mutated target site (Moses et al. 2010). However, this is still debated for the HIV LTR, since another study showed that siRNAs targeting HIV1 LTR are specific to the HIV1 LTR and does not affect the highly related HIV2 LTR neither a panel of other genes regulated in a similar way (Suzuki et al. 2011). However, to our knowledge, siRNAs targeting RNAs in regions far from their promoter and resulting in their promoter repression has not been reported so far.

Here, we show that siRNAs directed against a chromatin-associated RNA from the vlincRNA (very long intergenic non-coding RNA) family can silence its promoter even when targeting sequences are located thousands of bases downstream from the promoter. Moreover, through the use of genome edition, we found that this effect occurs in cis and is not due to off target mechanisms, therefore demonstrating the existence of RNA interference mechanisms acting at distance in mammals.

Results

siRNAs can efficiently decrease the expression of nuclear RNAs

In previous works, we successfully used siRNAs to deplete the expression of various RNAs associated with chromatin (Lazorthes et al. 2015; Muniz et al. 2017; Muniz et al. 2021). This includes depletion of an RNA we called VAD, a senescence-specific ncRNA which belongs to the vlincRNA family (Lazorthes et al. 2015). More recently, we investigated another senescence-specific ncRNA from the vlincRNA family, also strongly associated with chromatin and located in the vicinity of the *INK4* locus, that was unidentified so far and that we called VINK, for VlincRNA close to *INK4* (Ouvrard et al., in preparation). During the course of this investigation, we designed and transfected siRNAs directed against this vlincRNA in RAF1 oncogene-induced senescent WI38 human cells. By RT-qPCR, we observed that an siRNA against VINK (VINK-1 siRNA) efficiently inhibits VINK expression when measured at various places along the VINK RNA (Figure 1A and 1B). A similar result was obtained with a second independent couple of control and VINK siRNAs (VINK-2 siRNA), although VINK inhibition was slightly less efficient with this siRNA (Figure 1C). This efficient depletion using these two siRNAs was also observed on RNA-Seq experiments (Figure 1D). Thus, our siRNAs against the VINK vlincRNA efficiently repress VINK expression.

These data, as well as the data we previously published on other chromatin-associated RNAs (Lazorthes et al. 2015; Muniz et al. 2017; Muniz et al. 2021), were obtained in senescent WI38 cells expressing the hTERT, the catalytic subunit of the human telomerase and an ER-RAF1

fusion protein. To test whether the depletion of the chromatin-associated VINK RNA by siRNAs can be observed in other cell types, we made use of the human osteosarcoma U2OS cell line that also expresses VINK. In U2OS cells, transfection of siRNAs against VINK specifically and efficiently repressed VINK expression (Figure 1E).

Thus altogether, these data indicate that siRNAs can efficiently induce the knock-down of the chromatin-associated VINK RNA.

siRNAs affect the transcription of their targeted nuclear RNAs

Given that the use of siRNAs to target nuclear RNAs is debated, we intended to investigate the mechanism of this effect. To that goal, we analyzed whether siRNAs directed against VINK induced its degradation. We thus transfected senescent WI38 cells with the VINK-1 siRNA (which is the most efficient, see Figure 1B) or control siRNA and treated transfected cells with actinomycin D to block the transcription. The decrease of VINK expression along time reflects its stability. Using this experimental setting, we found that the half-life of VINK was between 100 and 200 minutes, depending on the region of VINK analyzed (Figure 2A). This half-life was longer when we analyzed the 5' extremity of VINK (VINK-A), probably because this part of VINK can be found in a more stable spliced form (Ouvrard et al., in preparation). Surprisingly, wherever investigated, VINK half-life was not changed in cells transfected with the VINK-1 siRNA. Moreover, no difference in its half-life was observed upon VINK-1 siRNA transfection following either short or long periods of actinomycin treatment (Figure 2A and S1). Thus, these experiments suggest that the stability of VINK RNA is not affected by the presence of VINK siRNAs.

We next assessed whether VINK siRNAs affected VINK transcription. To that goal, we analysed ongoing transcription by nascent RNA capture, which relies on metabolic labelling of RNAs being transcribed with a nucleotide analogue, allowing their biotinylation and purification on streptavidin beads. Analysis of recovered nascent RNAs thus provides an accurate measure of ongoing transcription. We transfected senescent WI38 cells with the two siRNAs against VINK and measured nascent transcripts at different locations along VINK (Figure 2B). We found that the presence of VINK nascent RNA was strongly decreased upon transfection of the two VINK siRNAs in all regions analyzed (Figure 2B). Thus, siRNAs targeting VINK RNA decrease its transcription, even when the RNA targeting sequences are far from the promoter and the transcription start site (TSS) (>20 kb and >200 kb). Importantly, this effect was also observed in U2OS cells (Figure 2C), indicating that it is not a specific feature of the WI38 cell line.

To test whether this effect is restricted to VINK or to RNAs from the vlincRNA family, we transfected senescent WI38 cells with a siRNA directed against the ARHGAP18 read-through RNA belonging to the family of START RNAs that we characterized in a previous study (Muniz et al. 2017). Read-through RNAs are produced by transcription beyond the transcription termination site and are known to be nuclear/chromatin associated (Vilborg et al. 2015). We also observed that the presence of ARHGAP18 START nascent RNA was strongly decreased upon transfection of the siRNA targeting it (Figure 2D). ARHGAP18 nascent transcript from which the START RNA originates was also decreased, as measured close to its TSS in its first exon and intron and 150 kb upstream the siRNA targeted site (Figure 2D). These results indicate that the effect of the siRNA directed against ARHGAP18 START RNA is also transcriptional. Thus, we conclude from these experiments that siRNAs can repress the transcription of the chromatin-associated RNA they target, even when the targeted site is far from the promoter.

siRNAs targeting VINK RNA influence RNA polymerase II presence at VINK TSS

Inhibition of nascent RNA upon siVINK transfection was observed throughout the VINK transcribed region, including when analyzing regions upstream of the siRNA-targeted sequence (Figures 1 and 2). This result suggests that VINK siRNA could affect the first steps of transcription occurring at VINK TSS and not transcription elongation. To analyze the step of transcription affected by siRNAs, we first analyzed the recruitment of RNA pol II to TSS. We thus transfected the VINK-1 or VINK-2 siRNAs and performed chromatin immunoprecipitation (ChIP) using an antibody that recognizes total RNA pol II. We found that both siRNAs against VINK inhibited the presence of RNA pol II at VINK TSS compared to control GAPDH TSS (Figure 3A, 3B and S2). We next analyzed whether it was also correlated with the regulation of chromatin marks. We found that the VINK-1 siRNA decreased the presence of the transcription-associated H3K27ac mark at VINK TSS (Figure 3C). Thus, these data indicate that siRNAs targeting VINK decrease the presence of transcription-associated chromatin marks and of RNA Pol II at VINK TSS, therefore decreasing VINK transcription. To our knowledge, this effect has never been reported so far with siRNAs targeting RNAs away from their promoter and TSS.

Repression of transcription by VINK siRNA is dependent on base-pairing to its target site

We next tested whether the effect of VINK siRNA on VINK transcription is due to base-pairing and not to off-target effects. Indeed, in some instances, transcriptional silencing using siRNAs was attributed to off-target effects (Moses et al. 2010).

To analyze whether pairing of the siRNA to its target site is involved, we raised, by genome edition in WI38 cells, a stable cell line that we called WI38-Δ/Δ #1, in which 210 bp encompassing the target site for the VINK-1 siRNA are deleted on the two alleles (see Figure S3 for the description of the cell line). We next transfected WI38-Δ/Δ #1 cells with the siRNAs directed against *VINK*. Whereas the VINK-2 siRNA works as in parental cells (compare Figures 4A and 1C), the VINK-1 siRNA, for which the sequence is not present in WI38-Δ/Δ #1 cells, did not repress VINK expression (Figure 4A). Importantly, a similar result was also observed in another independent clone deleted for the VINK-1-targeted sequence on the two alleles (WI38-Δ/Δ #2) (Figure 4B). The absence of effects of the VINK-1 siRNA on VINK expression in WI38-Δ/Δ #2 cells was also obvious from RNA-seq data when comparing the effect of the VINK-1 siRNA in parental WI38 (+/+) and deleted WI38-Δ/Δ #2 cells (Figure 4C).
Thus, removal of its target sequence abolished the effect of the VINK-1 siRNA on VINK expression, indicating that it represses the expression of its target RNA through base pairing to its target sequence.

VINK siRNA requires cis-targeting to repress transcription of VINK

All together the above-described data unambiguously demonstrate that the VINK-1 siRNA represses VINK transcription by a process involving base-pairing. This suggests that VINK-1

siRNA targets VINK RNA and induces chromatin modifications at VINK promoter in cis that would lead to the repression of transcriptional initiation. However, we cannot formally rule out the possibility that the VINK-1 siRNA targets and induces the degradation by conventional RNAi mechanisms of a sub-population of VINK, an effect that would not be observed in our previous experiments because it only represents a minor proportion of VINK. If this population was able to indirectly regulate VINK expression, its depletion could then be signalized to the VINK promoter to repress VINK transcription.

To formally demonstrate that the siRNA acts in cis, we raised by genome edition a cell line in which only one of the two alleles encoding VINK can be targeted by the VINK-1 siRNA (that we called WI38-Δ/+). If the effects of siRNAs were due to base pairing at chromatin inducing local chromatin modifications, only the siRNA-targeted allele would be repressed. On the contrary, if the repression of VINK transcription was indirect, then the two alleles should be depleted. We thus transfected WI38-Δ/+ cells with VINK-1 and VINK-2 siRNAs and performed RT-qPCR monitoring allele-specific VINK expression (see Figure 5A for the design of PCR primers). Both siRNAs inhibited the expression of the wild type allele, with, as in previous experiments (see Figure 1B-D), a higher effect of the VINK-1 siRNA compared to the VINK-2 siRNA (Figure 5B). In a striking contrast, on the deleted allele, we still observed repression by the VINK-2 siRNA, whereas repression by the VINK-1 siRNA was abolished (Figure 5C). The effect of the VINK-1 siRNA on total VINK expression in WI38-Δ/+ was weaker than on the wild type allele (compare Figure 5D with Figure 5B) or than in parental cells (compare Figure 5D with Figure 1B), as expected since only one allele was affected.
Altogether, these data thus demonstrate that the effect of VINK-1 siRNA on VINK transcription is mediated in *cis* by base-pairing of the siRNA to its target site on the chromatin-associated VINK RNA.

Ago1 and Ago2 are involved in siRNA-mediated VINK transcriptional repression

It was shown that transcriptional silencing by siRNA targeting promoters can involve either Ago1 or Ago2 (Janowski et al. 2006; Kim et al. 2006; Chu et al. 2010). We thus investigate whether these proteins also participate in the transcription repression by siRNAs targeting VINK body. To that goal, we made use of siRNAs targeting either Ago1 or Ago2. These two siRNAs were efficient and specific as observed by western blot (Figure 6A). We thus tested the effect of Ago1 and/or Ago2 knockdown on VINK repression by the VINK-1 siRNA. We found that siRNAs against Ago1 and Ago2 have a similar efficiency on their respective target whether or not they are transfected together with control siRNAs or siRNAs against VINK, indicating that transfection of many siRNAs together does not affect their efficiency (Figure 6B and C). In contrast, the effect of the VINK-1 siRNA was weaker in the presence of either Ago1 or Ago2 siRNA (Figure 6B) and was nearly abolished when knocking-down both Ago1 and Ago2 (Figure 6C). Thus, this result indicates that both Ago1 and Ago2 are involved in siRNA-mediated transcriptional repression of VINK.

Discussion

In this study, we show that siRNAs can induce efficient and specific transcriptional silencing of an RNA associated with chromatin. We observed this effect with siRNAs targeting the RNA far from the promoter that, to our knowledge, has never been described so far in mammals. We further demonstrate the involvement of Ago1 and Ago2 in this process. This silencing was lost when the sequences targeted by the siRNA were deleted, ruling out off-target effects and

demonstrating that base-pairing to its target sequence is required. Note that we cannot formally conclude whether this base pairing occurs on VINK RNA or on its transcribed template DNA.

The first question raised by our finding is whether the interference we have shown here with exogenously delivered siRNAs can also take place in natural conditions with endogenous siRNAs. Indeed, in various species, RNAi mechanisms have been shown to be involved in transcriptional silencing occurring at specific chromatin domains such as pericentric heterochromatin in fission yeast. Moreover, the involvement of endogenous antisense RNAs in the establishment or maintenance of heterochromatin silencing is well established (Lee and Lu 1999; Giles et al. 2010). Interestingly, it was recently proposed that tRNA-derived small RNAs (tsRNA) could be endogenous regulators of many genes, albeit by a different interference mechanism requiring cleavage by Ago2 (Di Fazio et al. 2022), and other examples of endogenous siRNAs produced from protein-coding gene bodies are described (Zhang et al. 2008). Thus, we can speculate that endogenous RNAs complementary to chromatin-associated RNAs could be important regulators of the expression of these RNAs in mammals by triggering RNAi and transcriptional gene silencing..

To our knowledge, our study is the first to show that interfering RNAs targeting a RNA in regions far from its promoter can induce its transcriptional silencing in mammals. Such long-distance effects have been widely described in other species, in particular in plants. In these cases, it relies on RNA-dependent RNA polymerase (RdRP) which mediates amplification and propagation of double strand RNAs towards the 5' end of RNAs (Castel and Martienssen 2013). However, in mammals, RdRP is not conserved. What could thus be the mechanism involved in the process we describe here? It is known that double strand RNAs targeting the vicinity of a promoter (upstream promoter or the first exon) can lead to transcriptional silencing of the

promoter through the induction of repressive epigenetic marks in a manner dependent on some RISC components (Castanotto et al. 2005; Suzuki et al. 2005; Weinberg et al. 2006). Here, we can speculate that the silencing of the promoter at distance of the siRNA target site could be achieved by chromatin folding that would bring the VINK/siRNA hybrid and the promoter in close proximity. Consequently, this would allow the establishment of repressive marks at the promoter, as proposed for miRNAs targeting the 3' end of genes (Yue et al. 2010; Younger and Corey 2011). This close proximity could be preexisting or induced by the presence of the double-stranded nucleic acids. The fact that we observe transcriptional silencing using many different siRNAs argues for this latter hypothesis. Note however, that we cannot exclude that the underlying mechanism involves propagation of double strand RNAs towards the 5' end of RNAs since a RdRP-like activity has been identified in human cells relying on TERT and RMRP (Maida et al. 2009).

Despite the fact that intronic sequences are also found associated with chromatin, siRNAs directed against intronic sequences of pre-mRNAs are usually not effective to decrease the expression of pre-mRNAs (Zeng and Cullen 2002; Vickers et al. 2003; Qiu et al. 2018). This finding first indicates that transcription of the target sequence is not sufficient to induce transcriptional silencing by siRNA, suggesting that the target of the siRNA is chromatin-associated RNA but not the DNA being transcribed. Splicing occurs co-transcriptionally leading to the degradation of introns, which thus greatly decrease the window of opportunity for the siRNA to bind efficiently its target RNA or to induce chromatin modifications when targeted. Moreover, siRNAs directed against a lncRNA did not induce transcriptional silencing, except when targeting the first exon (Stojic et al. 2016). Thus, whatever the mechanism involved, it

does not operate on any RNA associated with chromatin and we can speculate that the difference lies in the time of residence of the targeted RNA at chromatin.

The use of siRNAs to silence nuclear RNAs has been debated for long, because of the low levels of some RNAi proteins in the nucleus. As a consequence, siRNA-mediated degradation of RNA is mostly efficient in the cytoplasm. Nonetheless, as discussed above, siRNAs targeting promoters can in some instances repress transcription from the promoter they target. Here, we show that siRNAs targeting regions of chromatin-associated RNAs located far from the promoter can also silence transcription of targeted RNAs. Thus, siRNAs can represent interesting tools to investigate the function of chromatin-associated RNA by allowing their efficient and specific knock-down, even if the promoter is not well characterized or if the RNA is produced through multiple promoters. In addition, and coupled to a method allowing the degradation of RNA without interfering with any transcription step, it may help to distinguish between the role of the RNA itself and the role of its transcription, an ever-raising question in the field. Most importantly, since we found that siRNAs inhibit the transcription of the allele they target but not of the allele they do not target, they would allow studying *cis* effects of nuclear non coding RNAs or of their transcription, provided that an existing polymorphism or heterozygous genome edition, as we have done here, allows to target a single allele.

Note however that in the conditions we used to achieve the knock-down of VINK, VINK-1 siRNA induces prominent off-target effects with significant changes in the expression of hundreds of genes upon siRNA transfection in the cell line in which the target site of siRNA was deleted (Figure S4). Moreover, the use of two independent siRNAs was not sufficient to cope with off-target effects since most of the genes showing expression changes with two independent siRNA directed against VINK in wild type cells have a tendency to be changed in

a similar way in the cell line deleted for the siRNA target site (Figure S4B). These off-target effects are probably due to the fact that an siRNA can bind to and degrade target RNAs without perfect sequence complementarity, the seed region of only 6-7 nucleotides in the siRNA being involved in targeting numerous RNAs (Birmingham et al. 2006). It is possible that they are exacerbated when siRNAs do not have any target in the cytoplasm, such as for siRNAs directed against chromatin-associated RNAs or control siRNAs. Importantly, we have not been able to dissociate the base pairing-dependent repression of VINK expression to off-target effects by changing the amount of siRNAs or the time after transfection at which we harvested cells (data not shown). It will thus be critically important for functional studies to design an experimental strategy ruling out off-target effects, such as overexpression of a siRNA-resistant form of the targeted RNA, or, as we performed here, removal of the siRNA target site by genome edition. When possible, this latter strategy is probably better since it maintains the normal production of the RNA at the normal place in the genome and in the nucleus, which is sometimes critical for the function of non-coding RNAs.

Finally, our findings suggest that siRNAs targeting chromatin-associated RNAs may have therapeutic potential. Indeed, the therapeutic value of siRNAs is currently widely investigated. Moreover, the relation of chromatin-associated RNAs with cancer progression has been documented in many instances, such as PVT1, H19, MALAT1 and HOTAIR (for a recent review see (Chen et al. 2021)). RNAs from the vlincRNA family are also overexpressed in cancer cells (St Laurent et al. 2013), and this overexpression may participate in allowing these cells to survive genotoxic stress (Cao et al. 2021). Targeting these RNAs with siRNAs may thus have therapeutic potential. Moreover, by modifying the chromatin landscape at their promoters and thus potentially reversing epigenetic information, it may have long-term benefits.

Materials and Methods

Cell culture

WI38-hTERT/ER-RAF1 immortalized fibroblastic cell line was kindly provided by C. Mann (Jeanblanc et al. 2012). They were grown in MEM supplemented with L-glutamine, non-essential amino acids, sodium pyruvate, penicillin-streptomycin and 10% of fetal bovine serum under 5% CO2 and 5% O2. Senescence was induced by treating cells with 20 nM of 4-hydroxy-tamoxifen for three days. U2OS cells (ATCC) were grown in DMEM containing Glutamax supplemented with sodium pyruvate, penicillin-streptomycin and 10% of foetal bovine serum under 5% CO2. WI38 cells and derivatives were transfected using the siRNA transfection reagent Dharmafect 4 (Dharmacon) following the manufacturer's instructions with 100 nM of siRNA unless indicated in Figure legend and harvested 72 hours later. U2OS cells were transfected with the Interferin transfection reagent (Polyplus) or with Dharmafect 4 according to the manufacturers' instructions with 50 nM of siRNA and harvested 48 hours later. For RNA stability analysis, actinomycin D (Sigma) was added at 10 µg/mL. The list of siRNAs used are listed in Table S2.

Antibodies and western blots

Western blots were performed using standard protocols. Ago1 and Ago2 were detected using the monoclonal anti-AGO1 (6H1L4) antibody from Invitrogen (used at 1/1000) and the monoclonal anti-AGO2 (R.386.2) antibody from Invitrogen (1/1000), whereas GAPDH was

detected using the monoclonal anti-GAPDH (MAB374) antibody from Millipore (1/10000). The list of antibodies used in this study is shown in Table S4.

Genome Edition

Genome edition of WI38 was performed with CRISPR-Cas9 tools in ribonucleic particle (RNP) format. Briefly, the Alt-R S.p. HiFi Cas9 Nuclease V3 (IDT) was assembled with equimolar amount of hybridized sgRNA (tracrRNA and crRNA from IDT) to generate RNPs. According to IDT recommendations, RNPs were transfected at 5 nM each with Lipofectamine CRISPRMAX (Thermofisher). Cells were harvested one week later to analyse the efficiency of genome edition. Genomic DNA was extracted with Master Pure purification kit (Epicentre) according to the manufacturer's instructions, except that 250 µg of Proteinase K were used for cell lysis. Genome edition efficiency was checked by PCR on genomic DNA from the transfected population with the GoTaq G2 polymerase (Promega) using primers surrounding the 210 bp deleted region. PCR products were visualized on an agarose gel. Clones were then isolated and screened by PCR as described above. Two homozygous clones and one heterozygous clone were selected. The sequences of sgRNAs are indicated in Table S3.

RNA extraction, reverse transcription and qPCR

Except when indicated, total RNA was prepared using the MasterPure RNA Purification Kit (Epicentre) according to the manufacturer's instructions, except that 250 µg of Proteinase K was used for cell lysis. In some experiments, TRIzol (Sigma) was used. Briefly, adherent cells are directly lysed with 0.1 mL/cm^2 of TRIzol during 10 min, the lysate is harvested before adding 0.1 mL of chloroforme per mL of TRIzol. After centrifugation, the upper phase is

collected and the Epicentre kit is used for the following DNase digestion and subsequent precipitation. After total nucleic acids recovery, DNA was removed with a cocktail of DNaseI and Baseline Zero DNase supplemented with Riboguard RNase Inhibitor for 45 min at 37°C. 500 ng of total RNA were reverse transcribed with Superscript III reverse transcriptase (Invitrogen) according to manufacturer's instructions. A condition without Superscript III was performed for each sample and analysed by qPCR using GAPDH exon 9 primers to check for DNA contamination. qPCR was performed in triplicate with TB green Premix Ex Taq from Takara and the Biorad CFX thermocycler. GADPH mRNA expression was used to normalize the results of RT-qPCR. The primers used are indicated in Table S1.

Nascent RNA capture

Cells were incubated with 0.2 mM of ethynyl-uridine, a uridine analogue, for 1h. Cells were then harvested, total RNA was prepared and nascent RNA was purified from 2 µg of total RNA with the Click IT Nascent RNA capture kit from Life Technologies according to the manufacturer's recommendations.

Chromatin immunoprecipitation (ChIP)

ChIP was performed on 10.10^6 transfected senescent WI38 cells as previously described (Lazorthes et al. 2015), except that the nuclear lysis buffer was diluted twice before use, and sonicated nuclei were diluted 5 times in the dilution buffer. Briefly, 10 million cells transfected with siRNA were crosslinked for 15 min using 1% formaldehyde directly in the culture medium. 0.125 M of glycine were then added for 5 min. After two washes with PBS, cells were scraped and frozen at -80°C. Cells were lysed with 3 ml of lysis buffer (5 mM Pipes pH 8, 85

mM KCl, 0.5% NP40) and homogenized 40 times with a dounce (20 times, pause 2 minutes, 20 times). After centrifugation, nuclear pellets were resuspended in 1.5 ml of nuclear lysis buffer (25 mM Tris pH 8.1, 5 mM EDTA, 0.5% SDS), and sonicated 10 times for 5s (power setting 0.5 ON 0.5 OFF and 50% amplitude, Branson Sonifier 250), to obtain DNA fragments of about 500 bp. DNA concentration was determined using a Nanodrop and samples were adjusted to the same concentration of chromatin. Samples were diluted five times in dilution buffer (0.01% SDS, 1.1% Triton X-100, 1.2 mM EDTA pH 8, 17 mM Tris pH 8.1, 167 mM NaCl) and precleared for 2 h with 250 µL of previously blocked 50% protein-A and protein-G beads (Sigma P-7786 and P-3296 respectively). Blocking was achieved by incubating the beads with 0.5 mg/ml of Ultrapure BSA and 0.2 mg/mL of salmon sperm DNA for 4 h at 4°C. 100 µL of chromatin were kept for inputs. 100 µg of pre-cleared samples per ChIP were incubated overnight for RNA pol II ChIP or 40 µg for histones ChIP with 4µg of antibody at 4°C. A mock sample without antibody was processed similarly. Then, 40 µL of blocked 50% A/G beads were added for 2h at 4°C to recover immune complexes. Beads were washed once in dialysis buffer (2 mM EDTA, 50 mM Tris pH 8, 0.2% Sarkosyl), five times in wash buffer (100 mM Tris pH 8.8, 500 mM LiCl, 1% NP40, 1% NaDoc) and twice in TE buffer (10 mM Tris pH 8, 1 mM EDTA). The bead/chromatin complexes were resuspended in 200 µL of TE buffer and incubated 30 min at 37 °C with 10 µg of RNase A (Abcam), as well as input DNA. Formaldehyde crosslink was reversed in the presence of 0.2% SDS at 70°C overnight with shaking. After 2 h of proteinase K (0.2 mg/ml) treatment at 45°C, immunoprecipitated and input DNA were purified on columns using Illustra GFX kit (GE Healthcare). All buffers for ChIP experiment were supplemented with EDTA-free protease inhibitor cocktail (Roche) and filtered 0.2 µM. Results were analysed by qPCR. The list of primers and antibodies used is indicated in Table S1 and Table S4 respectively.

Statistics

In all figures with statistical analyses, data were normalized to 1 relative to a control which was included in each experiment (usually a control siRNA). For significance analysis, the Log2 of fold change compared to this control was calculated in order to obtain data with a normal distribution. All experiments were then pooled together to calculate the variance of these experiments with a sufficient number of points. We then calculated using the student t test with this fixed variance the probability that the mean of each data set is equal to 0 (the value of the control), which represents the p value of the difference to the control. In some cases, we calculated using the paired student t test the probability that the mean of two populations is equal, which represents the p value of the difference between the two populations. A star is included in the Figure when the p value is below 0.05. The p value is indicated in the figure when it is between 0.05 and 0.1. When above 0.1, the difference is considered as non-significant and "ns" is indicated.

RNA-seq

We performed strand-specific RNA-Seq method, relying on UTP incorporation in the second cDNA strand. For each sample, 5-10 µg of total RNA was submitted to EMBL-GeneCore, Heidelberg, Germany. Paired-end sequencing was performed by Illumina's NextSeq 500 technology. Two replicates of each sample were sequenced.

The quality of each raw sequencing file (fastq) was verified with FastQC (Andrews 2010). Files were aligned to the reference human genome (hg38) in paired-end mode with STAR Version 2.5.2b and processed (sorting and indexing) with samtools (Li et al. 2009). rDNA contamination was removed in the alignment process. Uniquely aligned reads were counted, per gene_id, using

HT-seq Version 0.6.1 in a strand specific mode with the union count method parameter (Anders et al. 2014). The features' annotation used for counts was constructed from NCBI refseq annotation gtf file from UCSC, taking the entire locus of reference for each gene. After removing lowly expressed counts (> 4 reads over the 4 samples), differential analysis was performed with DESeq2 Bioconductor R package, Version 1.22.1 (Love et al. 2014). Counts were normalized using DESeq2 normalization method. Both treatment (siRNA VINK/siRNA Ctrl) and batch (replicates) effects were taken into account to estimate parameters and fit the model, in order to apply Wald test. Bigwig files were generated using rtracklayer Bioconductor-R package, Version 3.10, with 1 base pair bining and normalization based on the total number of read aligned.

Data availability

RNA-Seq data are available in the Geo database under the accession number # GSE197308

Acknowledgements

This work was supported by a grant fom the Ligue Nationale Contre le Cancer to DT as an "équipe labellisée". JO is supported by studentships from the French Ministry of Science and from the Fondation pour la Recherche Médicale (FRM). LM was supported by a fellowship from the Fondation de France.

The authors wished to thank Antonin Morillon, Hervé Seitz and all members of D Trouche's lab for helpful discussions. This work was supported by a grant fom the Ligue Nationale Contre le Cancer to DT as an "équipe labellisée". JO is supported by studentships from the French Ministry of Science and from the Fondation pour la Recherche Médicale (FRM). LM was

supported by a fellowship from the Fondation de France. RNA-Seq data were analysed by the genomic facility (BigA) from the CBI.

References

Anders S, Pyl P, Huber W. 2014. HTSeq - A Python framework to work with high throughput sequencing data. *Bioinformatics* ***doi:10.1093/bioinformatics/btu638***.

Andrews S. 2010. FastQC: a quality control tool for high throughput sequence data. *Available online at :* *http://wwwbioinformaticsbabrahamacuk/projects/fastqc/*.

Benhamed M, Herbig U, Ye T, Dejean A, Bischof O. 2012. Senescence is an endogenous trigger for microRNA-directed transcriptional gene silencing in human cells. *Nat Cell Biol* **14**: 266-275.

Birmingham A, Anderson EM, Reynolds A, Ilsley-Tyree D, Leake D, Fedorov Y, Baskerville S, Maksimova E, Robinson K, Karpilow J et al. 2006. 3' UTR seed matches, but not overall identity, are associated with RNAi off-targets. *Nat Methods* **3**: 199-204.

Cao H, Xu D, Cai Y, Han X, Tang L, Gao F, Qi Y, Cai D, Wang H, Ri M et al. 2021. Very long intergenic non-coding (vlinc) RNAs directly regulate multiple genes in cis and trans. *BMC Biol* **19**: 108.

Castanotto D, Tommasi S, Li M, Li H, Yanow S, Pfeifer GP, Rossi JJ. 2005. Short hairpin RNA-directed cytosine (CpG) methylation of the RASSF1A gene promoter in HeLa cells. *Mol Ther* **12**: 179-183.

Castel SE, Martienssen RA. 2013. RNA interference in the nucleus: roles for small RNAs in transcription, epigenetics and beyond. *Nat Rev Genet* **14**: 100-112.

Chen Y, Li Z, Chen X, Zhang S. 2021. Long non-coding RNAs: From disease code to drug role. *Acta Pharm Sin B* **11**: 340-354.

Chu Y, Yue X, Younger ST, Janowski BA, Corey DR. 2010. Involvement of argonaute proteins in gene silencing and activation by RNAs complementary to a non-coding transcript at the progesterone receptor promoter. *Nucleic Acids Res* **38**: 7736-7748.

Di Fazio A, Schlackow M, Pong SK, Alagia A, Gullerova M. 2022. Dicer dependent tRNA derived small RNAs promote nascent RNA silencing. *Nucleic Acids Res* **50**: 1734-1752.

Gagnon KT, Li L, Chu Y, Janowski BA, Corey DR. 2014. RNAi factors are present and active in human cell nuclei. *Cell Rep* **6**: 211-221.

Giles KE, Ghirlando R, Felsenfeld G. 2010. Maintenance of a constitutive heterochromatin domain in vertebrates by a Dicer-dependent mechanism. *Nat Cell Biol* **12**: 94-99; sup pp 91-96.

Han J, Kim D, Morris KV. 2007. Promoter-associated RNA is required for RNA-directed transcriptional gene silencing in human cells. *Proc Natl Acad Sci U S A* **104**: 12422-12427.

Hawkins PG, Santoso S, Adams C, Anest V, Morris KV. 2009. Promoter targeted small RNAs induce long-term transcriptional gene silencing in human cells. *Nucleic Acids Res* **37**: 2984-2995.

Janowski BA, Huffman KE, Schwartz JC, Ram R, Hardy D, Shames DS, Minna JD, Corey DR. 2005. Inhibiting gene expression at transcription start sites in chromosomal DNA with antigene RNAs. *Nat Chem Biol* **1**: 216-222.

Janowski BA, Huffman KE, Schwartz JC, Ram R, Nordsell R, Shames DS, Minna JD, Corey DR. 2006. Involvement of AGO1 and AGO2 in mammalian transcriptional silencing. *Nat Struct Mol Biol* **13**: 787-792.

Jeanblanc M, Ragu S, Gey C, Contrepois K, Courbeyrette R, Thuret JY, Mann C. 2012. Parallel pathways in RAF-induced senescence and conditions for its reversion. *Oncogene* **31**: 3072-3085.

Kalantari R, Hicks JA, Li L, Gagnon KT, Sridhara V, Lemoff A, Mirzaei H, Corey DR. 2016. Stable association of RNAi machinery is conserved between the cytoplasm and nucleus of human cells. *RNA* **22**: 1085-1098.

Kim DH, Villeneuve LM, Morris KV, Rossi JJ. 2006. Argonaute-1 directs siRNA-mediated transcriptional gene silencing in human cells. *Nat Struct Mol Biol* **13**: 793-797.

Lazorthes S, Vallot C, Briois S, Aguirrebengoa M, Thuret JY, St Laurent G, Rougeulle C, Kapranov P, Mann C, Trouche D et al. 2015. A vlincRNA participates in senescence maintenance by relieving H2AZ-mediated repression at the INK4 locus. *Nat Commun* **6**: 5971.

Lee JT, Lu N. 1999. Targeted mutagenesis of Tsix leads to nonrandom X inactivation. *Cell* **99**: 47-57.

Li H, Handsaker B, Wysoker A, Fennel T, Ruan J, Homer N, Marth G, Abecasis G, Durbin R. 2009. The sequence alignment /Map (SAM) format and SAMtools. *BioinformaticsR and 1000 Genome Project Data Processing Subgroup* **25**: 2078-2079.

Liu J, Carmell MA, Rivas FV, Marsden CG, Thomson JM, Song JJ, Hammond SM, Joshua-Tor L, Hannon GJ. 2004. Argonaute2 is the catalytic engine of mammalian RNAi. *Science* **305**: 1437-1441.

Love MI, Huber W, Anders S. 2014. Moderated estimation of fold change and dispersion for RNA-seq data with DESeq2. *Genome Biol* **15**: 550.

Maida Y, Yasukawa M, Furuuchi M, Lassmann T, Possemato R, Okamoto N, Kasim V, Hayashizaki Y, Hahn WC, Masutomi K. 2009. An RNA-dependent RNA polymerase formed by TERT and the RMRP RNA. *Nature* **461**: 230-235.

Martinez J, Patkaniowska A, Urlaub H, Lührmann R, Tuschl T. 2002. Single-stranded antisense siRNAs guide target RNA cleavage in RNAi. *Cell* **110**: 563-574.

Meister G, Landthaler M, Patkaniowska A, Dorsett Y, Teng G, Tuschl T. 2004. Human Argonaute2 mediates RNA cleavage targeted by miRNAs and siRNAs. *Mol Cell* **15**: 185-197.

Morris KV, Chan SW, Jacobsen SE, Looney DJ. 2004. Small interfering RNA-induced transcriptional gene silencing in human cells. *Science* **305**: 1289-1292.

Moses J, Goodchild A, Rivory LP. 2010. Intended transcriptional silencing with siRNA results in gene repression through sequence-specific off-targeting. *RNA* **16**: 430-441.

Muniz L, Deb MK, Aguirrebengoa M, Lazorthes S, Trouche D, Nicolas E. 2017. Control of Gene Expression in Senescence through Transcriptional Read-Through of Convergent Protein-Coding Genes. *Cell Rep* **21**: 2433-2446.

Muniz L, Lazorthes S, Delmas M, Ouvrard J, Aguirrebengoa M, Trouche D, Nicolas E. 2021. Circular ANRIL isoforms switch from repressor to activator of p15/CDKN2B expression during Raf1 oncogene-induced senescence. *RNA Biol* **18**: 404-420.

Napoli S, Pastori C, Magistri M, Carbone GM, Catapano CV. 2009. Promoter-specific transcriptional interference and c-myc gene silencing by siRNAs in human cells. *EMBO J* **28**: 1708-1719.

Qiu L, Hu X, Jing Q, Zeng X, Chan KM, Han J. 2018. Mechanism of cancer: Oncohistones in action. *J Genet Genomics* **45**: 227-236.

Sarshad AA, Juan AH, Muler AIC, Anastasakis DG, Wang X, Genzor P, Feng X, Tsai PF, Sun HW, Haase AD et al. 2018. Argonaute-miRNA Complexes Silence Target mRNAs in the Nucleus of Mammalian Stem Cells. *Mol Cell* **71**: 1040-1050.e1048.

Schwartz JC, Younger ST, Nguyen NB, Hardy DB, Monia BP, Corey DR, Janowski BA. 2008. Antisense transcripts are targets for activating small RNAs. *Nat Struct Mol Biol* **15**: 842-848.

Sharma NR, Wang X, Majerciak V, Ajiro M, Kruhlak M, Meyers C, Zheng ZM. 2016. Cell Type- and Tissue Context-dependent Nuclear Distribution of Human Ago2. *J Biol Chem* **291**: 2302-2309.

St Laurent G, Shtokalo D, Dong B, Tackett MR, Fan X, Lazorthes S, Nicolas E, Sang N, Triche TJ, McCaffrey TA et al. 2013. VlincRNAs controlled by retroviral elements are a hallmark of pluripotency and cancer. *Genome Biol* **14**: R73.

Stojic L, Niemczyk M, Orjalo A, Ito Y, Ruijter AE, Uribe-Lewis S, Joseph N, Weston S, Menon S, Odom DT et al. 2016. Transcriptional silencing of long noncoding RNA GNG12-AS1 uncouples its transcriptional and product-related functions. *Nat Commun* **7**: 10406.

Suzuki K, Ishida T, Yamagishi M, Ahlenstiel C, Swaminathan S, Marks K, Murray D, McCartney EM, Beard MR, Alexander M et al. 2011. Transcriptional gene silencing of HIV-1 through promoter targeted RNA is highly specific. *RNA Biol* **8**: 1035-1046.

Suzuki K, Shijuuku T, Fukamachi T, Zaunders J, Guillemin G, Cooper D, Kelleher A. 2005. Prolonged transcriptional silencing and CpG methylation induced by siRNAs targeted to the HIV-1 promoter region. *J RNAi Gene Silencing* **1**: 66-78.

Ting AH, Schuebel KE, Herman JG, Baylin SB. 2005. Short double-stranded RNA induces transcriptional gene silencing in human cancer cells in the absence of DNA methylation. *Nat Genet* **37**: 906-910.

Vickers TA, Koo S, Bennett CF, Crooke ST, Dean NM, Baker BF. 2003. Efficient reduction of target RNAs by small interfering RNA and RNase H-dependent antisense agents. A comparative analysis. *J Biol Chem* **278**: 7108-7118.

Vilborg A, Passarelli MC, Yario TA, Tycowski KT, Steitz JA. 2015. Widespread Inducible Transcription Downstream of Human Genes. *Mol Cell* **59**: 449-461.

Weinberg MS, Villeneuve LM, Ehsani A, Amarzguioui M, Aagaard L, Chen ZX, Riggs AD, Rossi JJ, Morris KV. 2006. The antisense strand of small interfering RNAs directs histone methylation and transcriptional gene silencing in human cells. *RNA* **12**: 256-262.

White E, Schlackow M, Kamieniarz-Gdula K, Proudfoot NJ, Gullerova M. 2014. Human nuclear Dicer restricts the deleterious accumulation of endogenous double-stranded RNA. *Nat Struct Mol Biol* **21**: 552-559.

Younger ST, Corey DR. 2011. Transcriptional regulation by miRNA mimics that target sequences downstream of gene termini. *Mol Biosyst* **7**: 2383-2388.

Yue X, Schwartz JC, Chu Y, Younger ST, Gagnon KT, Elbashir S, Janowski BA, Corey DR. 2010. Transcriptional regulation by small RNAs at sequences downstream from 3' gene termini. *Nat Chem Biol* **6**: 621-629.

Zeng Y, Cullen BR. 2002. RNA interference in human cells is restricted to the cytoplasm. *RNA* **8**: 855-860.

Zhang MX, Ou H, Shen YH, Wang J, Coselli J, Wang XL. 2005. Regulation of endothelial nitric oxide synthase by small RNA. *Proc Natl Acad Sci U S A* **102**: 16967-16972.

Zhang MX, Zhang C, Shen YH, Wang J, Li XN, Chen L, Zhang Y, Coselli JS, Wang XL. 2008. Effect of 27nt small RNA on endothelial nitric-oxide synthase expression. *Mol Biol Cell* **19**: 3997-4005.

Figure legends

Figure 1 - Small interfering RNAs can efficiently decrease VINK expression

A: Schematic representation of VINK genomic localisation, with siRNA binding sites and qPCR primers localisation indicated. **B**: Senescent WI38-RAF1 cells were transfected with the VINK-1 or control (Ctle-1) siRNAs. 72 hours later, total RNA was prepared and analysed by RT-qPCR for the expression of GAPDH mRNA or VINK (using the indicated primers). The amount of VINK RNA was standardized to GAPDH mRNA and calculated relative to 1 for cells transfected with the Ctle-1 siRNA. The means and standard deviations from 5 independent experiments are shown. *: p value < 0.05 compared to control. **C**: Same as in B, except that siVINK-2 and another control siRNA (Ctle-2) were used. The means and standard deviations from 7 independent experiments are shown. *: p value < 0.05 compared to control. **D**: WI38-RAF1 cells were treated as in B and C, and total RNA was analysed by RNA-Seq. Two duplicates of RNA-seq experiments were visualized in the IGB browser showing the normalized read coverage for the VINK locus. **E**: U2OS cells were transfected with the indicated siRNAs. 48 hours later, total RNA was prepared and analysed by RT-qPCR for the expression of GAPDH mRNA or VINK (using the indicated primers). The amount of VINK RNA was standardised to GAPDH mRNA and calculated relative to 1 for cells transfected with the Ctle-1 siRNA. The means and standard deviations from 3 independent experiments are shown. *: p value < 0.05 compared to Ctle-1 siRNA ; ns: non-significant, p value > 0.1.

Figure 2 - Small interfering RNAs affect VINK transcription

A: Senescent WI38-RAF1 cells were transfected with the VINK-1 or control (Ctle-1) siRNAs. 48 hours later, actinomycin D (10 µg/mL) was added or not. Cells were harvested after the indicated time. Total RNA was prepared and analysed by RT-qPCR for the expression of GAPDH mRNA or VINK (using the indicated primers). The amount of VINK RNA was standardised to GAPDH mRNA and calculated relative to 100 for the untreated sample. The means and standard deviations from 3 independent experiments are shown. Student t test was performed to compare VINK1 or Ctle-1 siRNAs samples at each time point of actinomysin treatment. ns: p value > 0.1. **B**: Senescent WI38-RAF1 cells were transfected with the indicated siRNAs. Nascent RNAs (Biotin-pull down) were prepared and analysed by RT-qPCR for the expression of GAPDH mRNA or VINK (using the indicated primers). The amount of VINK RNA was standardised to GAPDH mRNA and calculated relative to 1 for the Ctle-1 siRNA. The means and standard deviations from 3 independent experiments are shown. *: p value < 0.05 compared to Ctle-2 siRNA. **C**: Same as in B, except that U2OS cells were used. *: p value < 0.05 compared to Ctle-1 siRNA ; ns: non-significant, p value > 0.1. **D**: Senescent WI38-RAF1 cells were transfected with Ctle-1 siRNA or an siRNA directed against ARHGAP18 START RNA (Muniz et al. 2017). Nascent RNAs (Biotin-pull down) were prepared and analysed by RT-qPCR for the expression of GAPDH mRNA or the indicated primers on ARHGAP18. The amount of ARHGAP18 or START RNA was standardised to GAPDH mRNA and calculated relative to 1 for the Ctle-1 siRNA. The means and standard deviations from 3 independent experiments are shown. *: p value < 0.05 compared to Ctle-1 siRNA ; ns: non-significant, p value > 0.1; number: p value compared to Ctle-1 siRNA.

Figure 3 – VINK siRNAs affect the presence of RNA polymerase II at VINK promoter

A: Schematic representation showing the localization of the TSS (transcriptional start site) of VINK and primers used to analyse ChIP experiments. **B**: Senescent WI38-RAF1 cells were transfected with the indicated siRNAs. 72 hours later, fixed chromatin was prepared and subjected to a ChIP experiment using an antibody directed against total RNA pol II or no antibody as a control, as indicated. The amount of VINK TSS sequence was measured by qPCR with the indicated primers, standardized to the amount of GAPDH TSS sequence and calculated relative to 1 for the RNA pol II ChIP from cells transfected by the Ctle-1 siRNA. The means and standard deviations from four independent experiments are shown. Similar data with another VINK siRNA are shown in Fig. S2. *: p value < 0.05 compared to Ctle-2 siRNA. **C**: Same as in B, except that an anti-H3K27ac antibody was used. The amount of VINK TSS sequence is standardised to the amount of GAPDH TSS sequence and to nucleosome occupancy measured by ChIP using an antibody recognising total histone H3. The result is calculated relative to 1 for the H3K27ac ChIP from cells transfected by the Ctle-1 siRNA. The means and standard deviations from three independent experiments are shown. Number : p value compared to Ctle-2 siRNA.

Figure 4 – The siRNA target site is required for VINK repression

A: Senescent WI38-Δ/Δ #1 cells were transfected with the indicated siRNAs. 72 hours later, total RNA was prepared and analysed by RT-qPCR for the expression of GAPDH mRNA or VINK (using the indicated primers). The amount of VINK RNA was standardized to GAPDH mRNA and calculated relative to 1 for cells transfected with the Ctle-1 siRNA. The means and standard deviations from 3 independent experiments are shown. *: p value < 0.05 compared to Ctle-2 siRNA ; ns: non-significant, p value > 0.1. **B**: Same as in A, except that senescent WI38-Δ/Δ #2 cells were used. The means and standard deviations from five independent experiments

are shown. *: p value < 0.05 compared to Ctle-2 siRNA ; ns: non-significant, p value > 0.1; number: p value compared to Ctle1 siRNA. **C**: Senescent parental WI38-RAF1 (WI38-RAF1 WT) or WI38-Δ/Δ #2 cells were transfected with the indicated siRNA, and total RNA was analysed by RNA-Seq. Two duplicates of RNA-seq data for the VINK locus are shown. Note that data from WI38-RAF1 WT are the same as the four upper lines in Figure 1D.

Figure 5 - VINK siRNA requires a cis-targeting to chromatin to repress VINK transcription

A: Schematic representation of the two alleles of VINK present in WI38-Δ/+ with primers allowing their specific detection. The deleted allele is recognized by a primer located on the deletion junction. **B**: Senescent WI38-Δ/+cells were transfected with the indicated siRNAs. 72 hours later, total RNA was prepared and analysed by RT-qPCR for the expression of GAPDH mRNA or VINK wild type allele. The amount of VINK allele was standardised to GAPDH mRNA and calculated relative to 1 for cells transfected with the Ctle-2 siRNA. The means and standard deviations from 3 independent experiments are shown. *: p value < 0.05 compared to Ctle-2 siRNA ; ns: non-significant, p value > 0.1. **C**: Same as in B, except that the deleted VINK allele was analysed. The means and standard deviations from 3 independent experiments are shown. *: p value < 0.05 compared to Ctle-2 siRNA ; ns: non-significant, p value > 0.1; number: p value compared to Ctle2 siRNA. **D**: Same as in B and C, except that total VINK expression was analysed with the indicated primers. The means and standard deviations from 3 independent experiments are shown. *: p value < 0.05 compared to Ctle-2 siRNA ; ns: non-significant, p value > 0.1; number: p value compared to Ctle2 siRNA.

Figure 6 – Ago1 and Ago2 are involved in VINK transcriptional repression by VINK siRNA

A: Senescent WI38 cells were transfected with 30 nM of the indicated siRNAs. 72 hours later, cells were harvested and total cell extracts were subjected to a western blot analysis with antibodies directed against Ago1, Ago2 or GAPDH as a loading control. The stars (*) indicate non-specific bands. Identical results were obtained in three independent experiments **B**: Senescent WI38 cells were transfected with 30 nM of the indicated siRNAs. The amount of siRNAs was kept constant at 60 nM using Ctle-1 siRNA. 72 hours later, total RNA was prepared and analysed by RT-qPCR for the expression of GAPDH, Ago1 or Ago2 mRNA or VINK. The amount of Ago1, Ago2 or VINK were standardised to GAPDH mRNA and calculated relative to 1 for cells transfected with the Ctle-1 siRNA. The means and standard deviations from 3 independent experiments are shown. The significance of the difference in the fold change observed upon sVINK1 transfection in the absence or presence of Ago siRNAs was assessed by a paired student t test. *: p value < 0.05 compared to siVINK1 siRNA alone. **C**: Senescent WI38 cells were transfected with 25 nM of the indicated siRNAs. The amount of siRNAs was kept constant at 75 nM using Ctle-1 siRNA. 72 hours later, total RNA was prepared and analysed by RT-qPCR for the expression of GAPDH, Ago1 or Ago2 mRNA or VINK. The amount of Ago1, Ago2 or VINK were standardised to GAPDH mRNA and calculated relative to 1 for cells transfected with the Ctle-1 siRNA. The means and standard deviations from 6 independent experiments are shown. The significance of the difference in the fold change observed upon sVINK1 transfection in the absence or presence of Ago siRNAs was assessed by a paired student t test. *: p value < 0.05 compared to siVINK1 siRNA alone.

Figure S1 – Effect of longer actinomycin D treatment on VINK expression.

A Senescent WI38-RAF1 cells were transfected with the VINK-1 or control (Ctle-1) siRNAs. 48 hours later actinomycin D (10 µg/mL) was added or not. Cells were harvested after the indicated time. Total RNA was prepared and analysed by RT-qPCR for the expression of GAPDH mRNA or VINK (using the indicated primers). The amount of VINK RNA was standardized to GAPDH mRNA and calculated relative to 100 for the untreated sample. The means and standard deviations from 3 independent experiments are shown.

Figure S2 – The presence of RNA polymerase II at VINK TSS is also affected by the siVINK-2. Senescent WI38-RAF1 cells were transfected with the indicated siRNAs. 72 hours later, fixed chromatin was prepared and subjected to a ChIP experiment using an antibody directed against total RNA pol II or no antibody as a control, as indicated. The amount of VINK TSS sequence was measured by qPCR, standardized to the amount of GAPDH TSS sequence and calculated relative to 1 for the RNA pol II ChIP from cells transfected by the Ctle-1 siRNA. Error bars represent standard deviation of technical measurements (qPCR triplicates). Two entirely independent experiments are shown.

Figure S3 - Removal of siVINK-1 target site by CRISPR-Cas9-mediated genome edition. **A**: Schematic representation of the edited region, indicating the two guides inducing the deletion of 210 bp encompassing the siVINK-1 target site. **B**: Genome edition was checked by PCR on genomic DNA with primers located outside the deleted region. These primers produce a 420 bp fragment with the wild type allele and a 210 bp fragment with the deleted allele. The gel shows PCR results for parental cells (WT), the two cell lines with the two alleles deleted (Δ/Δ #2 and Δ/Δ #1) and the heterozygous cell line (Δ/+). **B**: Image of RNA-Seq from wild type

or Δ/Δ #2 cells showing the coverage around the region deleted in the Δ/Δ #2 cell line. Note the absence of reads in the deleted sequence in the RNA-Seq from the Δ/Δ #2 cells.

Figure S4 - VINK siRNAs induce prominent and reproducible direct or indirect off-target effects.

A: Senescent wild type WI38 cells were transfected with siVINK-1, siVINK-2, siCtle-1 and siCtle-2, whereas homozygously deleted (Δ/Δ #2) cells were transfected with siVINK-1 and siCtle-1. Total RNAs were prepared from two independent experiments and analysed by RNA-Seq. Differential gene expression (DGE) was performed with the DESeq2 package. The Table shows the numbers of significantly deregulated genes between siVINK and siCtle samples, as indicated, taking into account either only siVINK-1 and siCtle-1 samples or all four siRNAs for wild type cells. The numbers of deregulated genes intersected between wild type and Δ/Δ #2 cells are also indicated. Note that 2216 genes were significantly deregulated by the VINK1 siRNA in the Δ/Δ #2 cell line in which its target sequence as been deleted, thus representing off-target genes. Moreover, nearly half (1665) of the 3920 genes with significant changes in their gene expression upon VINK-1 siRNA transfection in the wild-type cell line are also significantly changed upon VINK-1 siRNA transfection in the deleted cell line. Similarly, 720 out of the 1616 genes significantly deregulated by the VINK1 and VINK2 siRNAs in wild type cells are also significantly changed upon VINK-1 siRNA transfection in the deleted cell line. Note that these off-target effects are not specific to the siRNA directed against VINK because control siRNAs that do not target any sequence in the genome, similarly induce off-targets effects (with 2165 DE genes between two different Ctrl siRNA samples, not shown in the table).

B: Scatter plot with the 1605 genes significantly deregulated by the two siVINK in wild type cells and expressed in the Δ/Δ #2 cells plotting the log2 of the fold change between siVINK-

1/siCtle-1 in the mutant (Y axis) and in the wild type (X-axis) cells. Note the strong correlation between the two datasets (R^2=0.707), indicating that many genes identified as deregulated by two independent siRNAs in wild type cells are similarly deregulated in Δ/Δ #2 cells, and are thus probably due to off-target effects.

Supplementary Table S1 – List of primers

Primers name	Sequences
VINK-A	FW: CTGGACACACCCTAGGCAAG RV: ATCCCTGTTGGTTATTCACAGC
VINK-B	FW: CCACAACCCCCATCTCTCTG RV: CCCATCTTTGGTTCTTCTGTC
VINK-C	FW: TGGGTAGCATCTTCATCGGTG RV: GAAGTGAGGGGAGTAGACAAG
VINK-D	FW: ACGCATGGGTGCCCTGTTTG RV: ATAGATCTTGGAGGGTGCCAG
VINK-E	FW: ACCACTATACAATTGCAGCAGG RV: CTGTCTGTTTAGGTACCTGGC
VINK-F	FW: GAGTGTCATCAGTAGTCTTAGCC RV: CGAGGTCCAATATCCCTAACC
420 bp encompassing the deletion product PCR primers	FW: GCATGAGTCATCTGGCTGTG RV: CCCATCTTTGGTTCTTCTGTC
WT VINK allele primers	FW: CCACAACCCCCATCTCTCTG RV: CCCATCTTTGGTTCTTCTGTC
Δ VINK allele primers	FW: ATATAGGAGGCCAGTGCTCCCCATG RV: CCCATCTTTGGTTCTTCTGTC
GAPDH exon 9 primers	FW: TGACAACGAATTTGGCTACAGC RV: CTCTTCCTCTTGTGCTCTTGC
GAPDH promoter primers	FW: AAATTGAGCCCGCAGCCTCC RV: GCGACGCAAAAGAAGATGCG
ARHGAP18-EX1	FW: CAGGCGAGACAGGAACTTCTTT RV: CTGCCTTTGCATGGCTGTTC

ARHGAP18-INT1	FW: GCTGCTGGAGTGAAATGTGG RV: TGTTCAGCTAGTGAGAAGGTC
ARHGAP18-read_through	FW: GTTCCTAGAGATTGATCTGAGG RV: GAATAGACTTGGGTTGCCACG
AGO1	FW: CAGTGGACACCAACATCACC RV: AAACGGTTGTCATCCCAAAG
AGO2	FW: CGCGTCCGAAGGCTGCTCTA RV: TGGCTGTGCCTTGTAAAACGCT

Supplementary Table S2 – List of siRNAs

siRNAs name	Sequences
siCtle-1	S: GUCAGAGUAUCAUACGUAA-UU AS: P-UUACGUAUGAUACUCUGAC-UU
siCtle-2	S: GACACAGUUCGAGUACUAA-UU AS: P-UUAGUACUCGAACUGUGUC-UU
siVINK-1	S: CUUCUCAAGUUUCGAACAA-UU AS: P-UUGUUCGAAACUUGAGAAG-UU
siVINK-2	S: GGGAAGGUAAGGAAAGAAA-UU AS: P-UUUCUUUCCUUACCUUCCC-UU
siARHGAP18-read_through	S: GGGCAGAGACUGAGACUUU-UU AS: P-AAAGUCUCAGUCUCUGCCC-UU
siAgo1	S: CCCAGAUACUCCACUAUGA–UU AS: P-UCAUAGUGGAGUAUCUGGG-UU
siAgo2	S: GGGUAAAGUUUACCAAAGA–UU AS: P-UCUUUGGUAAACUUUACCC-UU

Supplementary Table S3 – List of sgRNAs

sgRNAs name	Target Sequence
sgRNA-1	TAGGAGGCCAGTGCTCCAGG
sgRNA-2	TTCCTGACTCTTGAAAACCA

Supplementary Table S4 – List of antibodies

Antibody name	Reference
Anti-RNA pol II	A304-405A (Bethyl lab)
Anti-H3	Ab1791 (Abcam)
Anti-H3K27ac	Ab4729 (Abcam)
Anti-AGO1	6H1L4 (Invitrogen)
Anti-AGO2	R.386.2 (Invitrogen)
Anti-GAPDH	MAB374 (Millipore)

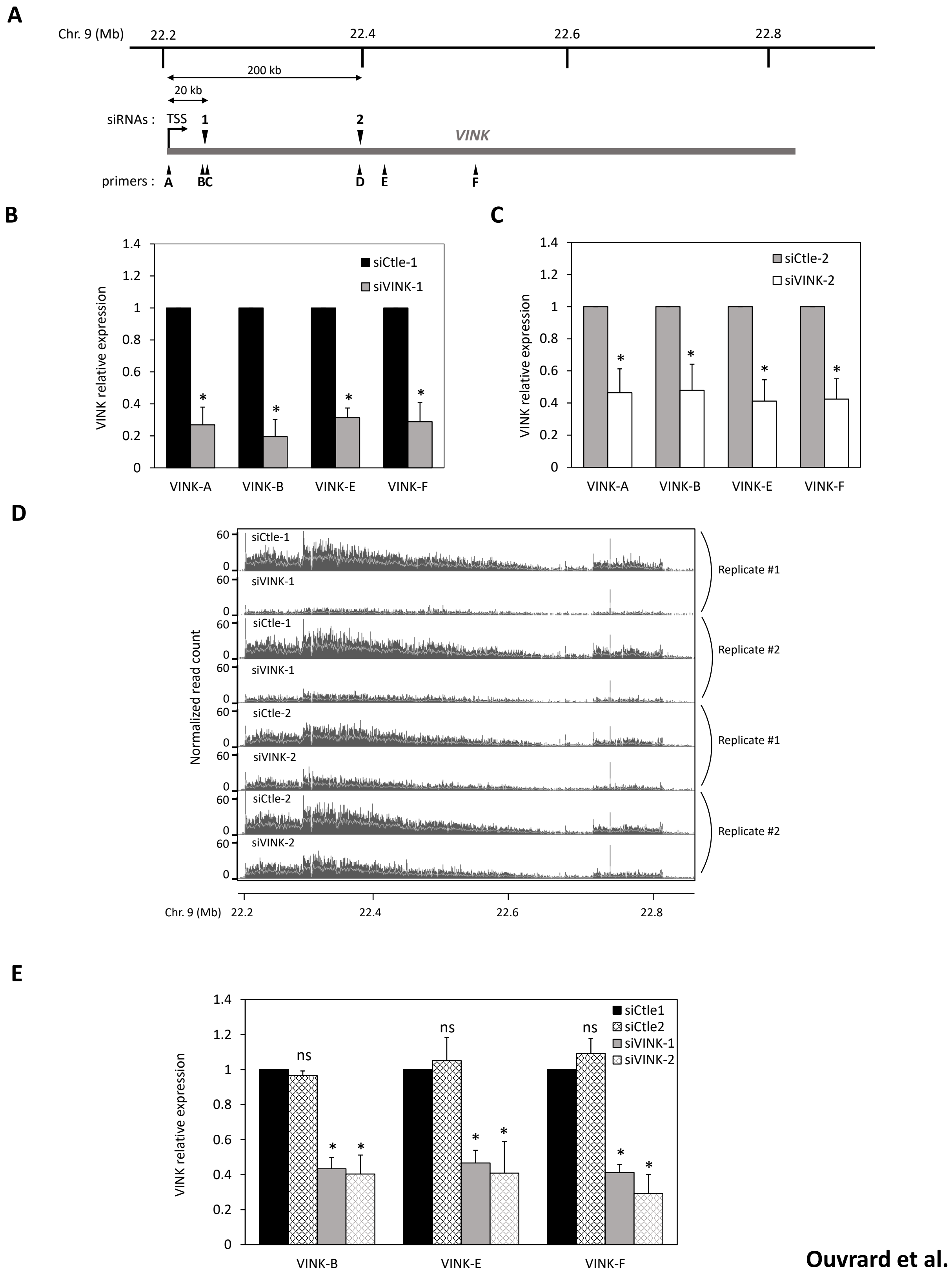

Ouvrard et al.
Figure 1

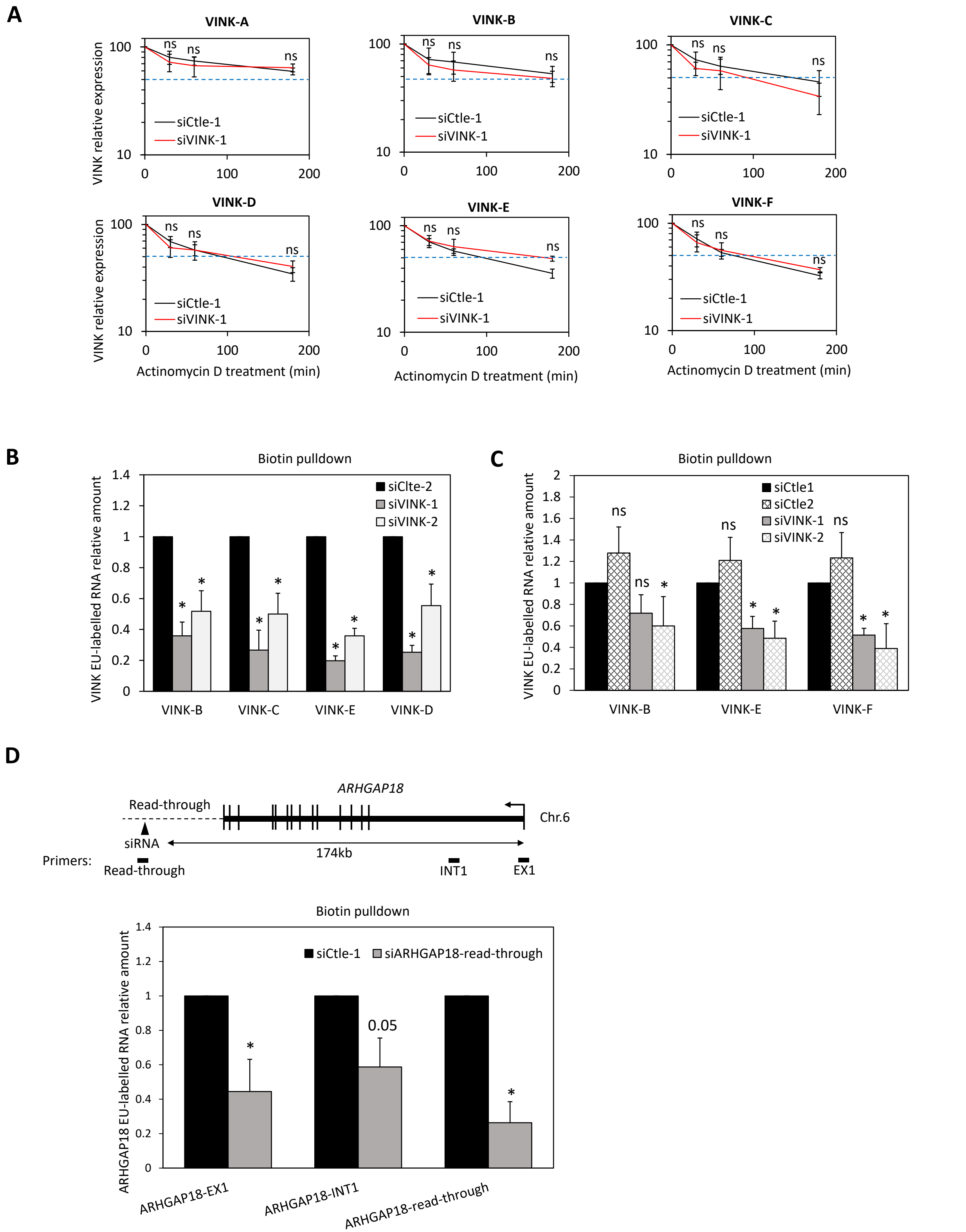

Ouvrard et al.
Figure 2

A

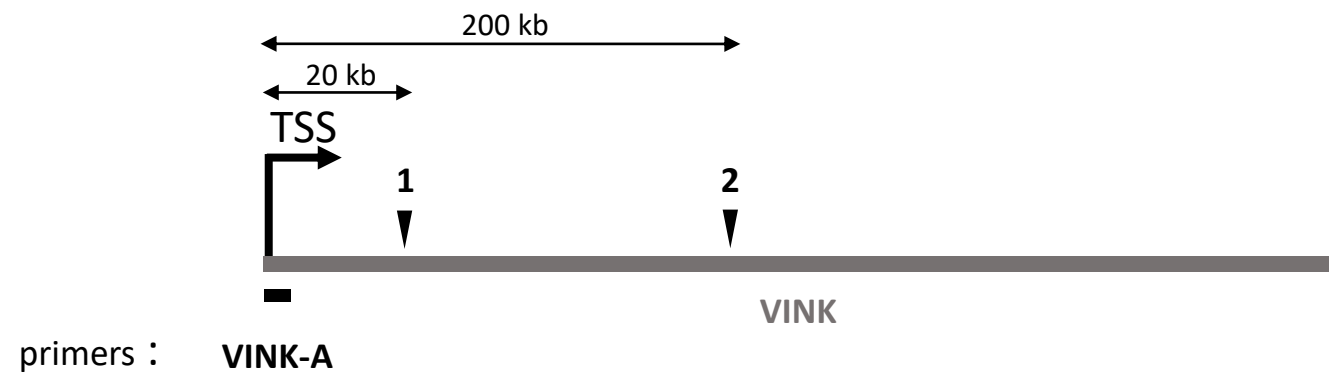

B

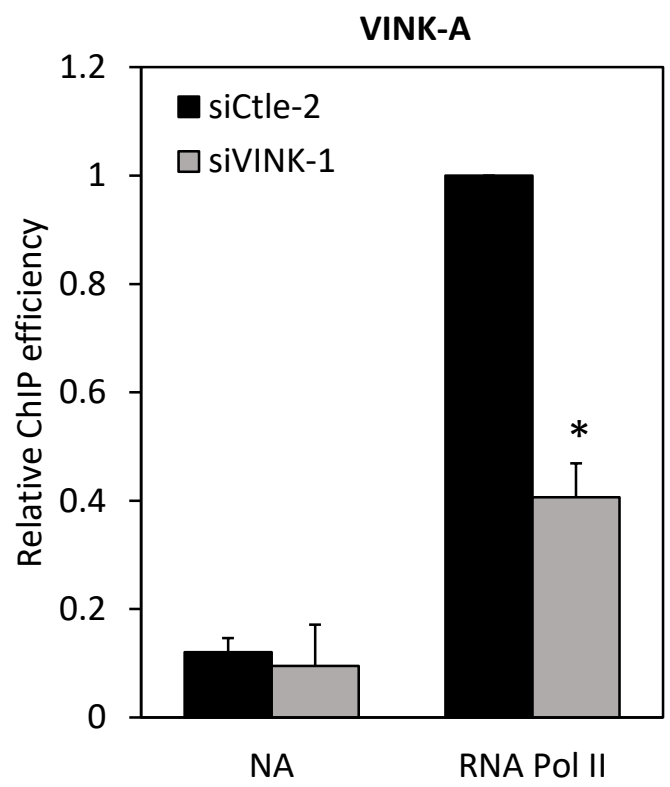

C

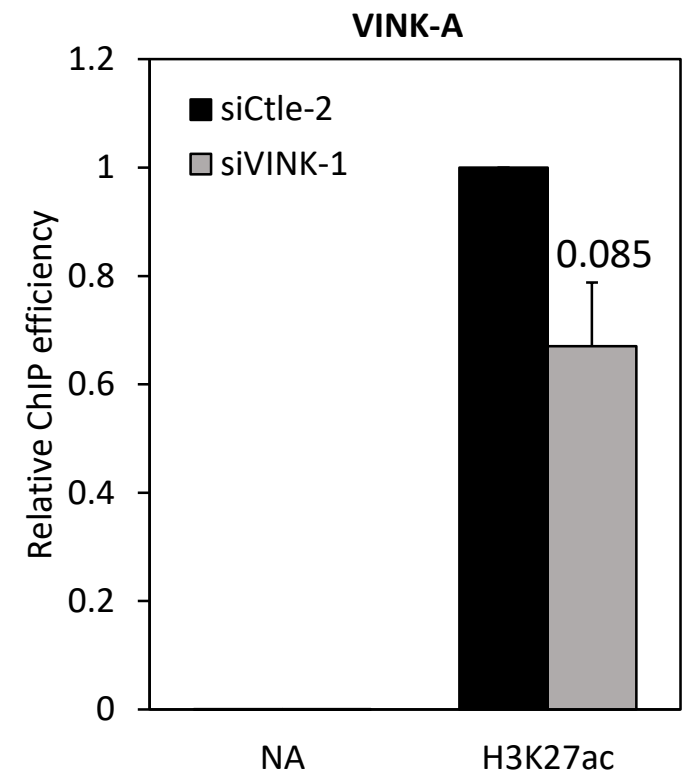

Ouvrard et al.
Figure 3

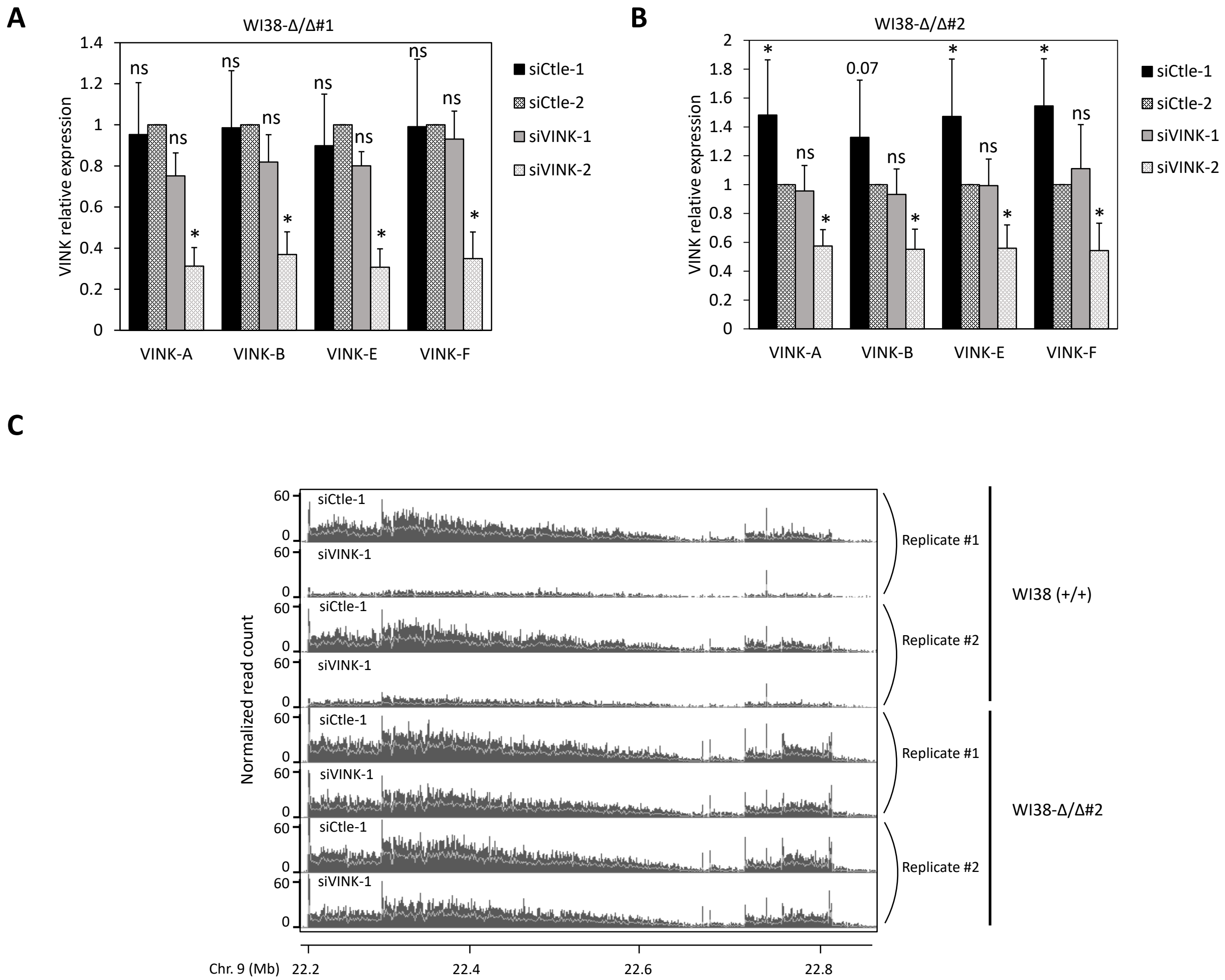

Ouvrard et al.
Figure 4

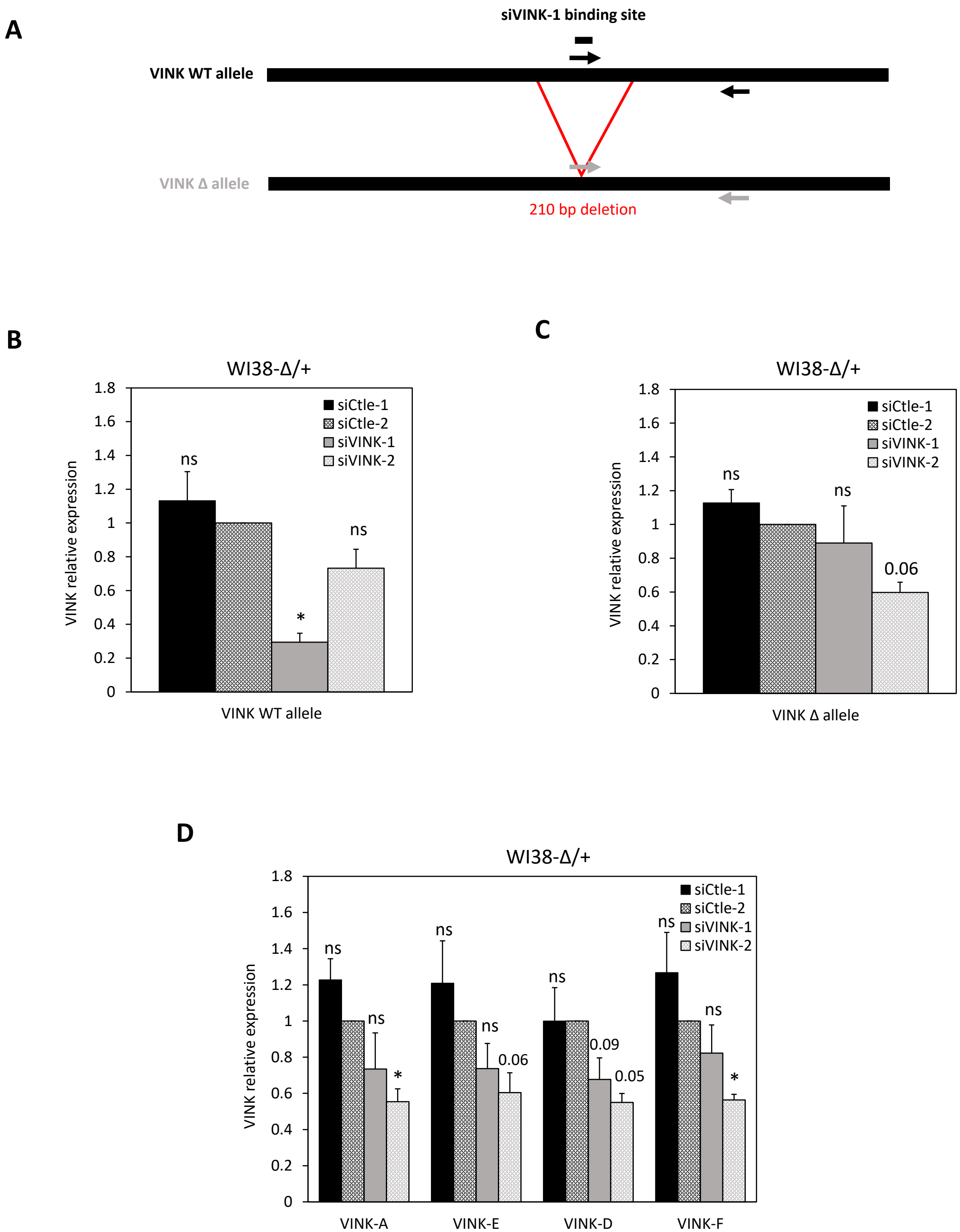

Ouvrard et al.
Figure 5

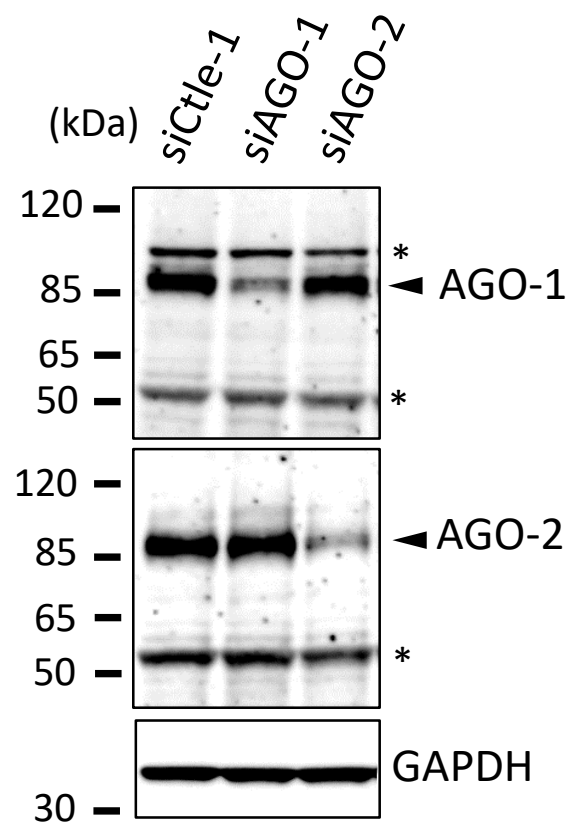

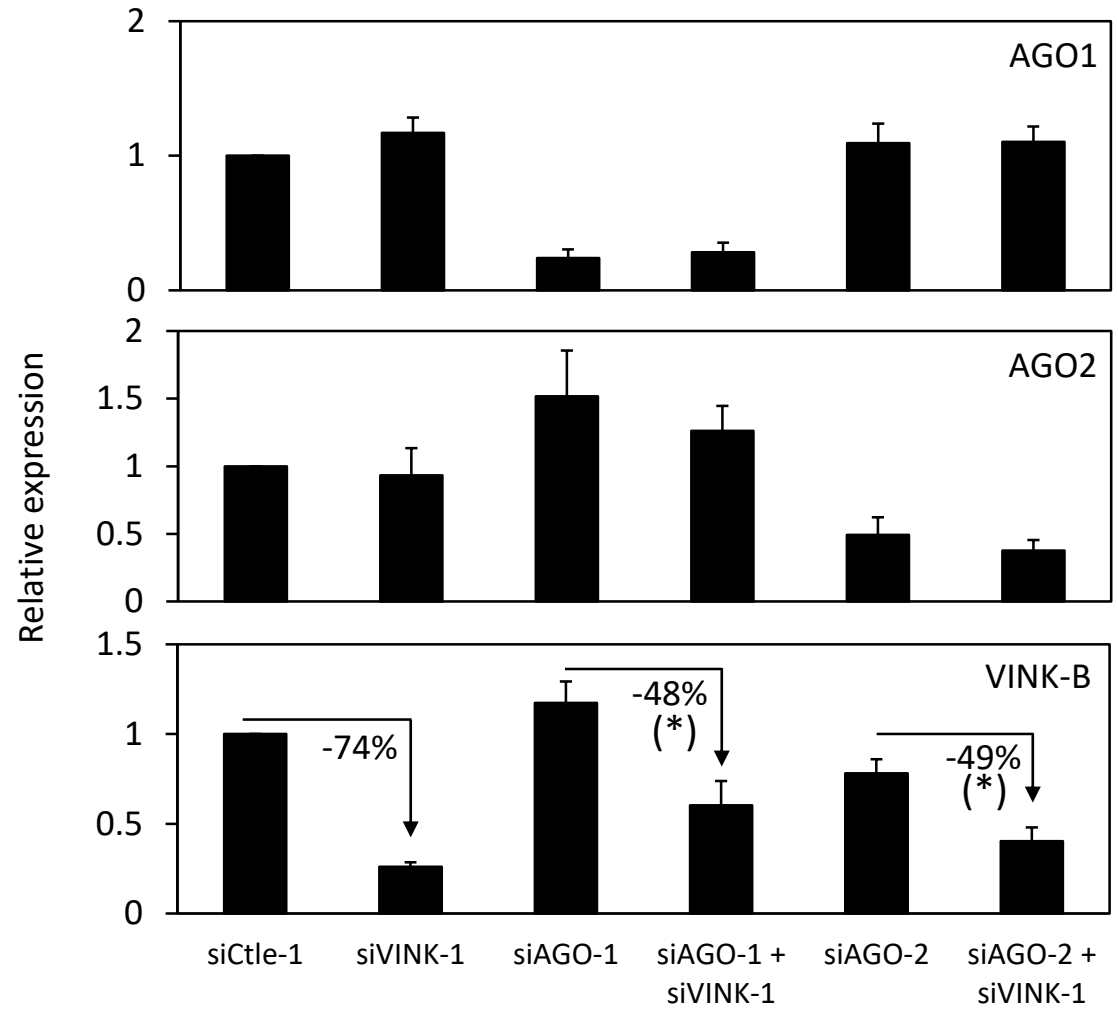

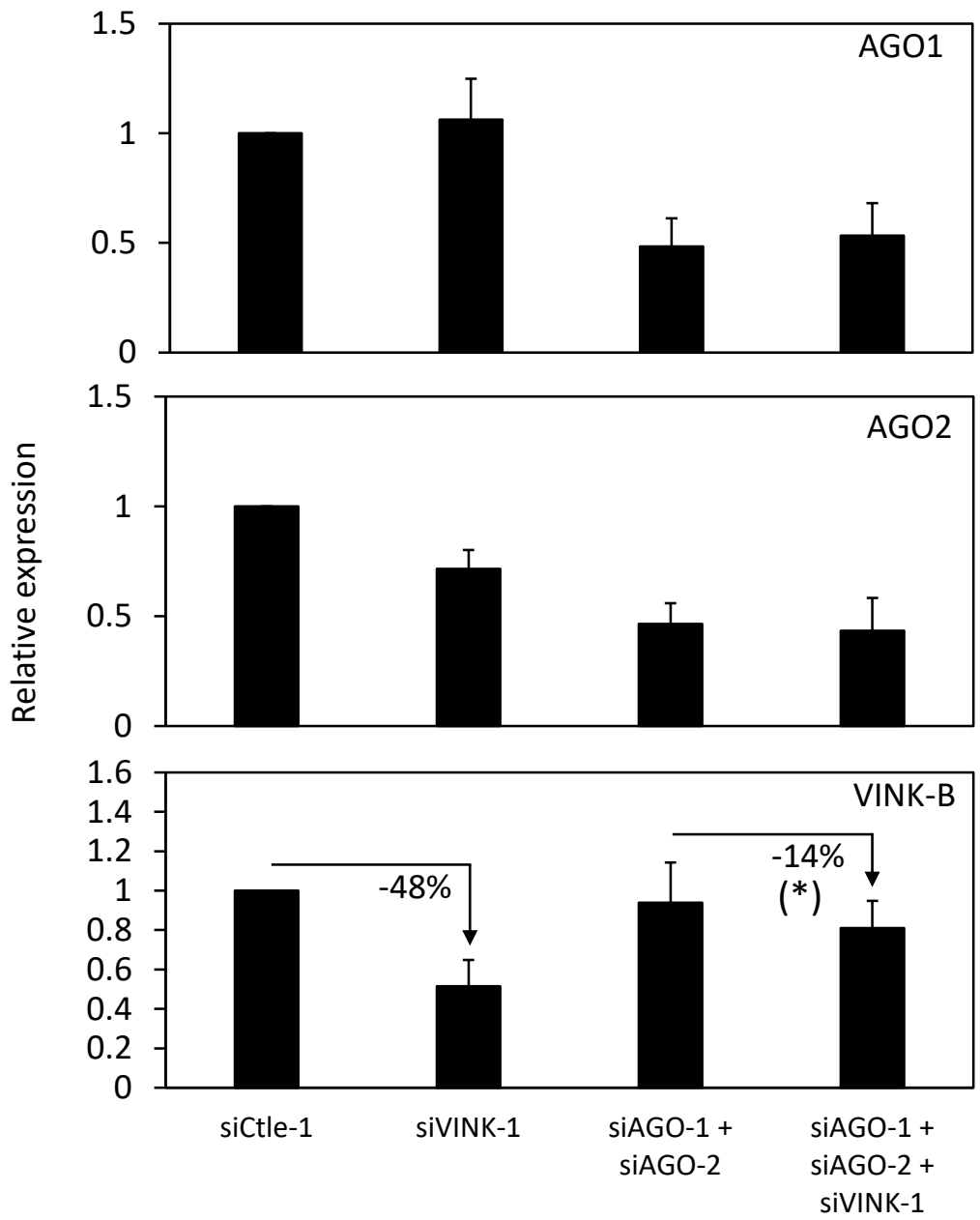

Ouvrard et al.
Figure 6

Figure S1 – Effect of longer actinomycin D treatment on VINK expression

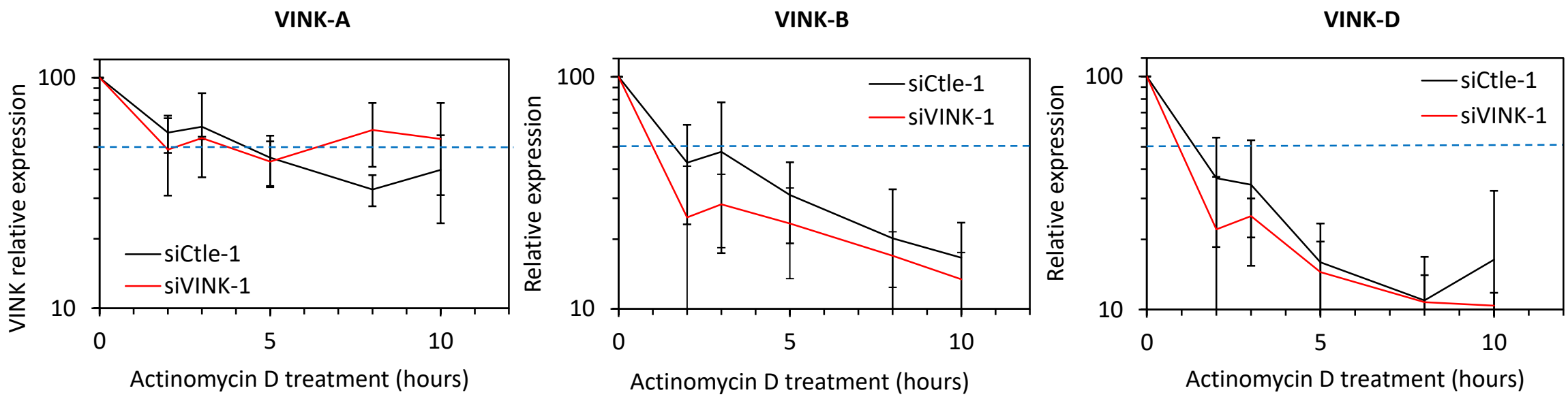

Figure S2 – The presence of RNA polymerase II at VINK TSS is also affected by the siVINK-2

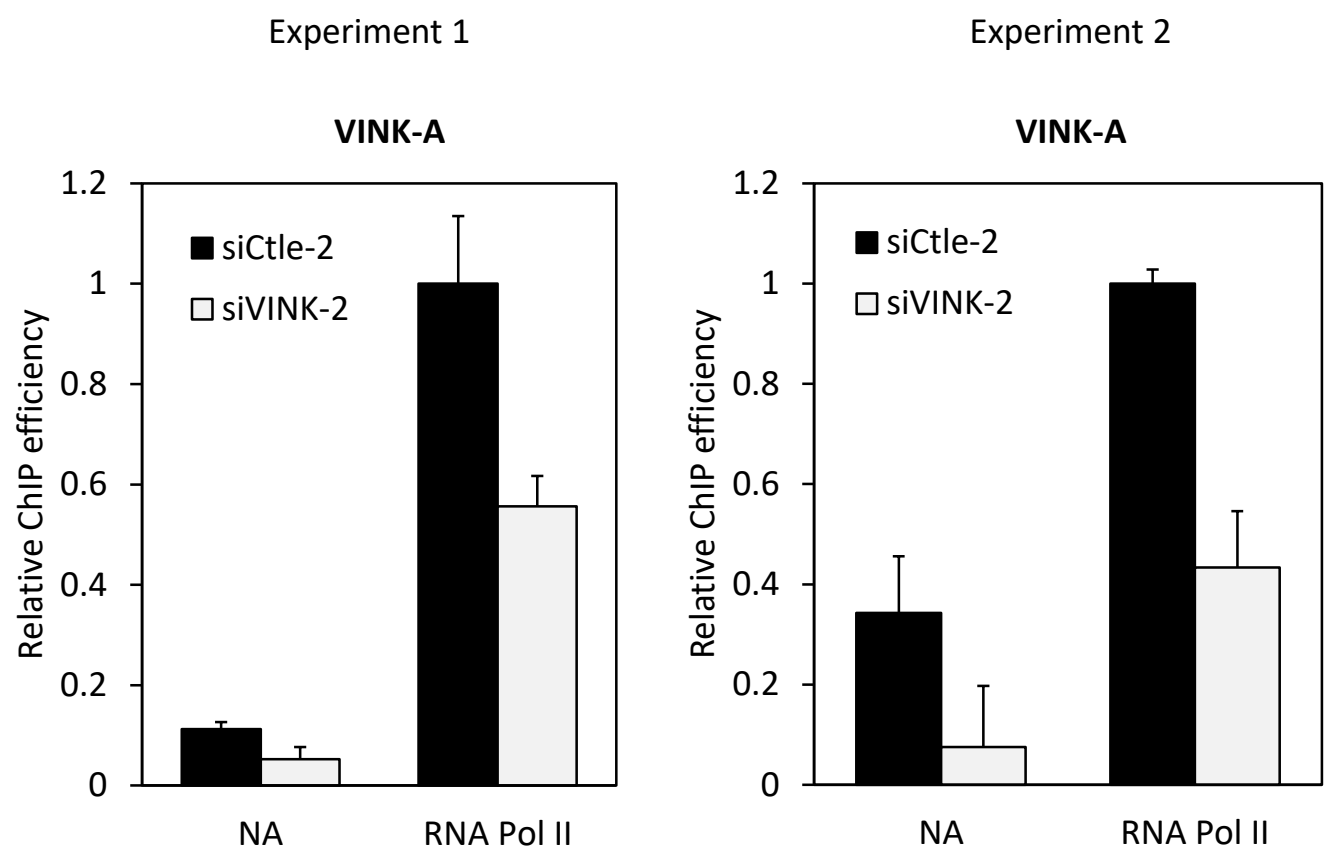

Figure S3 – Removal of siVINK-1 target site by CRISPR-Cas9-mediated genome edition

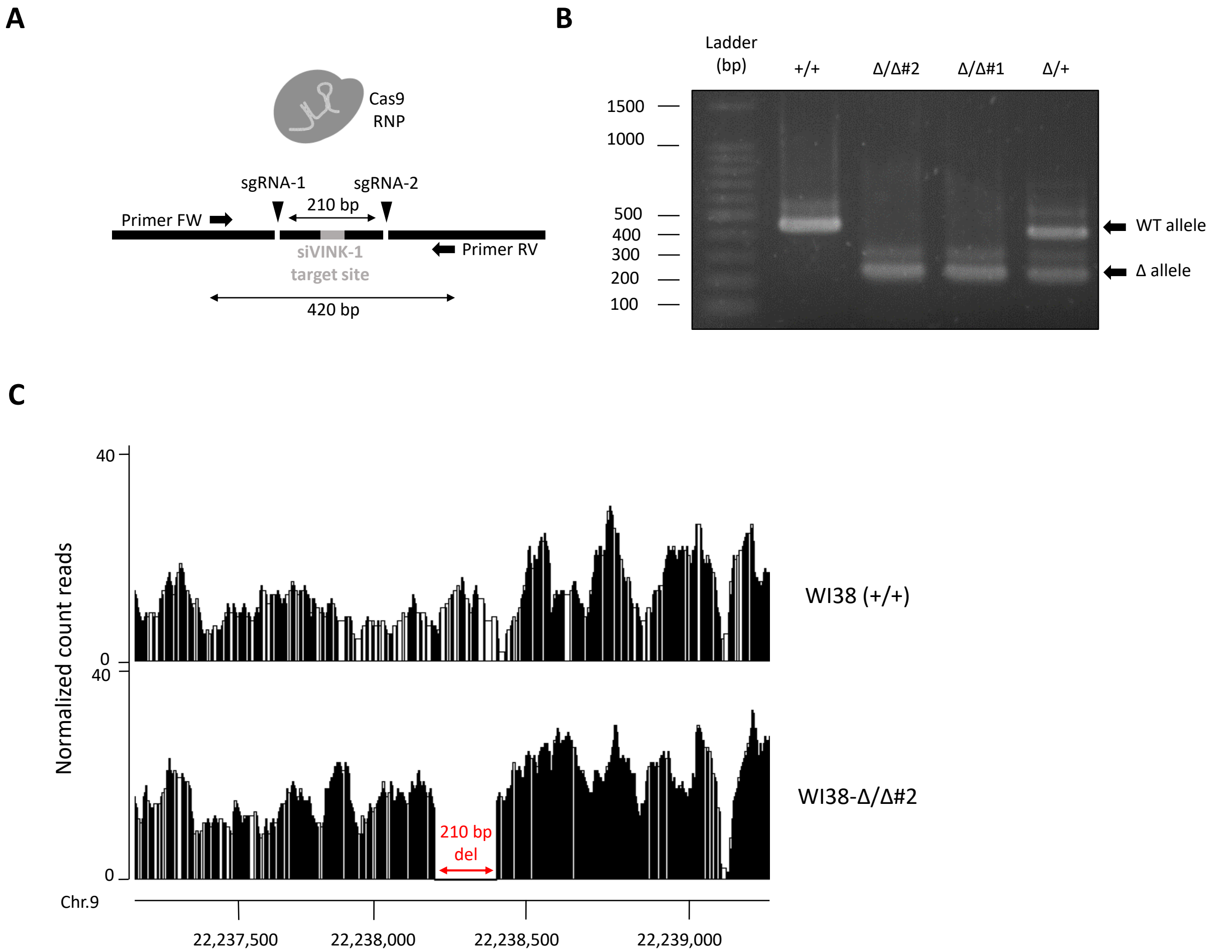

Figure S4 – VINK siRNAs induce prominent and reproducible direct or indirect off-target effects

A

DESEQ2 analysis

	DGE n°1 WI38-(+/+) (siVINK-1/siCtle-1)	DGE n°2 WI38-(+/+) (2 siVINK/2 siCtle)	DGE n°3 WI38-Δ/Δ#2 (siVINK-1/siCtle-1)	Common genes between DGE n°1 and n°3	Common genes between DGE n°2 and 3
Significant regulated genes (padj <0.05)	3920	1616	2216	1665	720
Down-regulated genes	2144	930	1313		
Up-regulated genes	1776	686	903		
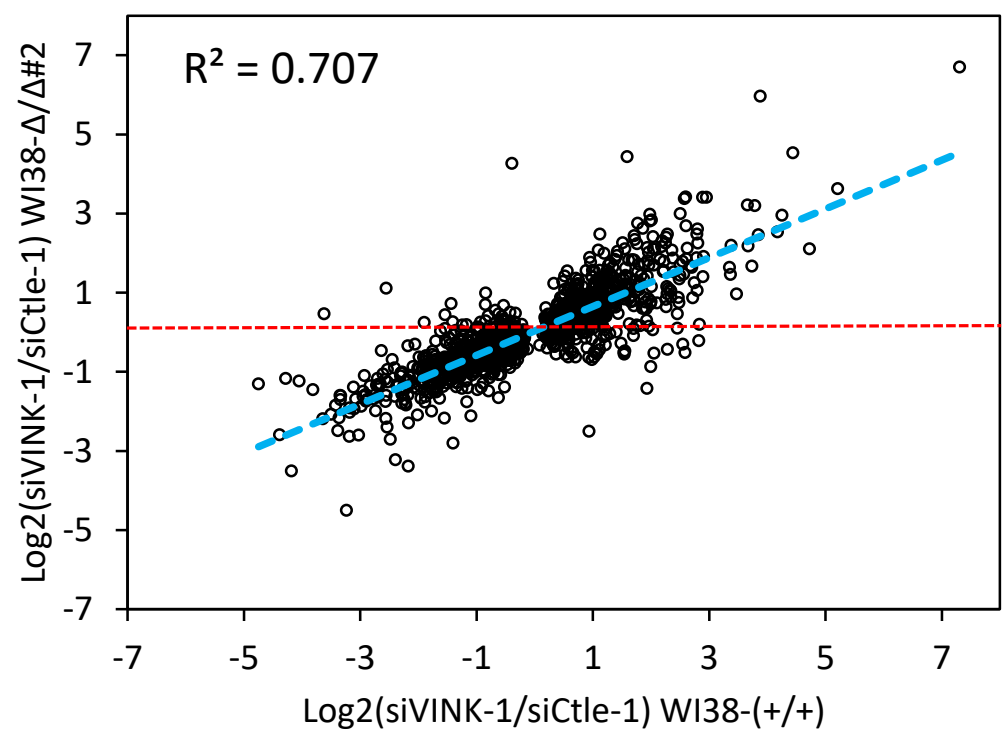
B